Experimental and Theoretical Investigation of the Charge-Separation Energies of Hydrated Zinc(II): Redefinition of the Critical Size

Theresa E. Cooper and P. B. Armentrout*

Department of Chemistry, University of Utah, 315 S. 1400 E. Rm 2020, Salt Lake City, Utah 84112

Received: July 2, 2009; Revised Manuscript Received: October 22, 2009

In the preceding article, the hydration energies of $Zn^{2+}(H_2O)_n$ complexes, where $n = 6-10$, were measured using threshold collision-induced dissociation (CID) in a guided ion beam tandem mass spectrometer (GIBMS) coupled with an electrospray ionization (ESI) source. The present investigation explores the charge-separation processes observed, $Zn^{2+}(H_2O)_n \rightarrow ZnOH^+(H_2O)_m + H^+(H_2O)_{n-m-1}$, and the competition between this process and the loss of water. Our results demonstrate that charge-separation processes occur at variable complex sizes of $n = 6$, 7, and 8, prompting a redefinition of the critical size for charge separation. Experimental kinetic energy-dependent cross sections are analyzed to yield 0 K threshold energies for the charge-separation products and the effects of competition with this channel on the energies for losing one and two water ligands after accounting for multiple collisions, kinetic shifts, and energy distributions. A complete reaction coordinate is calculated for the $n = 7$ complex dissociating into $ZnOH^+(H_2O)_3 + H^+(H_2O)_3$. Calculated rate-limiting transition states for $n = 6-8$ are also compared to experimental threshold measurements for the charge-separation processes.

Introduction

As detailed in the preceding article (article 1),[1] the zinc ion is required for the activation of certain proteins and metalloenzymes[2−4] and is used heavily in industry as well.[5] Because of its heavy usage, zinc is quickly infiltrating aqueous environments such that a complete understanding of the hydration of zinc(II) cations is essential to understand their behavior in aqueous environments. Zinc coordination and hydration behavior has previously been studied using a variety of experimental and theoretical methods,[6−19] as detailed in article 1.

In article 1,[1] the dissociation behavior of $Zn^{2+}(H_2O)_n$ complexes where $n = 7-10$ was examined using guided ion beam tandem mass spectrometry (GIBMS). In all cases, the dominant process observed is reaction 1,

$$Zn^{2+}(H_2O)_n \rightarrow Zn^{2+}(H_2O)_{n-1} + H_2O \quad (1)$$

followed by sequential loss of additional water molecules. Analysis of the kinetic energy dependence of these reactions provides the first experimental determinations of the hydration energies of zinc cation−water complexes. Article 1 shows that accurate thermochemistry relies on including consideration of different isomers, specifically how many inner-shell (x) versus outer-shell (y) water ligands are present in the reactants and products. These isomers are indicated by (x, y) nomenclature. Competing with reaction 1 is the charge-separation process, reaction 2.

$$Zn^{2+}(H_2O)_n \rightarrow ZnOH^+(H_2O)_m + H^+(H_2O)_{n-m-1} \quad (2)$$

This phenomenon has previously been examined using tandem mass spectrometry by Shvartsburg and Siu, who defined the critical size, n_{crit}, as "the maximum number of ligands at which dissociative charge transfer is competitive with simple ligand loss."[10] They found a lower limit to the critical size of Zn^{2+} complexes of $n_{crit} = 6$, whereas Blades et al. found $n_{crit} = 5$, also using CID studies.[11] Both reports suggest that the critical size depends directly on the second ionization energy of the metal. In related work, Peschke et al. found that when NH_3 vapor was added to $Zn^{2+}(H_2O)_n$ ($n = 8$ and 9), proton transfer to NH_3 and the formation of $ZnOH^+(H_2O)_m$ occurred with a dominant product of $m = 4$. Further addition of NH_3 vapor results in the formation of $ZnOH^+(NH_3)_m$ via ligand exchange.[7]

In the present work, we examine the competition between reactions 1 and 2, thereby providing more accurate thermodynamic information for both channels. Interestingly, we find that the charge-separation process, reaction 2, is observed for complexes of $n = 6$, 7, and 8, which to our knowledge, is the first time such a variable critical size has been observed for any metal. Given this ambiguity, we suggest that the energetics for reaction 2 can be used to provide a more exact definition of the critical size.

Experimental and Theoretical Section

Experimental Procedures. The experimental methods used to form $Zn^{2+}(H_2O)_n$ complexes and obtain their kinetic energy-dependent cross sections for collision-induced dissociation are described in detail in article 1.[1]

Threshold Analysis. Competition between the loss of water ligands, reaction 1, and the charge-separation process, reaction 2, from $Zn^{2+}(H_2O)_n$ can be modeled statistically, as discussed elsewhere, using eq 3 for an individual reaction channel, j,[20]

$$\sigma_j(E) = \frac{N\sigma_{0,j}}{E}\sum_i g_i \int_{E_{0,j}-E_i}^{E} \frac{k_j(E^*)}{k_{tot}(E^*)} P_{D1}(E - \varepsilon)^{N-1}\, d\varepsilon \quad (3)$$

where $\sigma_{0,j}$ is an energy-independent scaling factor for channel j, N is an adjustable parameter that describes the efficiency of

10.1021/jp906241q CCC: $40.75
Published on Web 11/11/2009

collisional energy transfer,[21] E is the relative kinetic energy of the reactants, $E_{0,j}$ is the threshold for CID of the ground electronic and rovibrational state of the reactant ion at 0 K for channel j, and ε is the energy transferred into the reactant ion by the collision such that the energy available for dissociation is $E^* = \varepsilon + E_i$. $P_{D1} = 1 - \exp[-k_{tot}(E^*)\tau]$ is the probability of dissociation of the energized molecule, EM, where τ is the experimental time-of-flight (5×10^{-4} s in this apparatus) and the rate constant, $k_{tot}(E^*)$, is given by Rice-Ramsperger-Kassel-Marcus (RRKM) theory,[22,23] as given by eq 4.

$$k_{tot}(E^*) = \sum k_j(E^*) = \sum s_j N^{\dagger}_{vr,j}(E^* - E_{0,j})/h\rho_{vr}(E^*) \quad (4)$$

Here, s_j is the reaction degeneracy of the dissociation channel j given by the ratio of the rotational symmetry numbers (reactant/products),[22] $N^{\dagger}_{vr,j}$ is the number of rovibrational states of the transition state (TS) for channel j at an energy $E^* - E_{0,j}$ above the reaction barrier, and $\rho_{vr}(E^*)$ is the density of states for the rovibrational levels of the EM. The incorporation of $k_j(E^*)$ and $k_{tot}(E^*)$ into eq 3 is discussed in detail elsewhere,[24−26] but allows modeling of the competition between channels and kinetic shifts resulting from complexes that are sufficiently large that their dissociation lifetime near the dissociation threshold is comparable to or longer than the experimental time-of-flight.

The rotational constants and vibrational frequencies of the EM and TSs are taken from quantum chemical calculations. As discussed previously for water loss channels,[1] the transition state is loose and treated at the phase space limit (PSL) in which the transitional modes are treated as rotors.[26] Thus, molecular parameters for these TSs are just those of the products and are taken from quantum chemical calculations detailed in article 1, as are molecular parameters for the EMs. Because the charge-separation process 2 produces two singly charged species, there must be a Coulombic barrier along the reactant coordinate for this dissociation channel, such that the appropriate TS is tight. Molecular parameters for these TSs are taken from calculations described below. TSs are labeled according to the products formed, that is, TS[$m + (n - m - 1)$] for the rate-limiting TS of reaction 2.

Both the primary dissociation of reaction 1 and subsequent loss of additional water molecules are influenced by competition with reaction 2 and vice versa. In the present work, the analysis of sequential dissociation channels includes the competition of the primary channel with reaction 2. The statistical approach to modeling sequential dissociation has recently been developed[27] and is described briefly in article 1.

Analysis of the data involves using eq 3 to reproduce the data over extended energy and magnitude ranges, using a least-squares criterion for optimizing the fitting parameters, $\sigma_{0,j}$, $E_{0,j}$, and N. The uncertainties in these parameters include variations associated with modeling several independent experimental cross sections, scaling the quantum chemical vibrational frequencies by ± 10%, varying the N value by ± 0.1, scaling the experimental time-of-flight up and down by a factor of 2, and the uncertainty in the absolute energy scale.

Computational Details. Using the *Gaussian03* package,[28] vibrational frequencies, rotational constants, and energies were calculated for all reaction species. The tight TSs of the charge-separation processes were found through a series of relaxed potential energy scans along the likely reaction coordinate at a B3LYP/6-31G(d) level.[29−31] Geometry optimizations and frequency calculations of the TSs and intermediates (INT) were performed at a B3LYLP/6-311+G(d,p) level. Here, the vibrational frequencies of the TSs were found to have only one imaginary frequency, and all INTs were determined to be vibrationally stable. These calculated frequencies and rotational constants were used in the RRKM thermochemical analysis discussed above, as well as for zero point energy (ZPE) conversions of theoretical bond dissociation energies to 0 K thermochemical values. The vibrational frequencies were scaled by 0.989[32] before being used in these analyses. Using these geometries, single point energy (SPE) calculations were performed using the B3LYP, B3P86,[33] and MP2(full)[34] levels with a 6-311+G(2d,2p) basis set.

Because of the importance of proton-bound water clusters in the present study, the computational procedure used here was tested by comparison with results from a previous experimental study of the solvation enthalpies of protonated water clusters, $H^+(H_2O)_z \rightarrow H^+(H_2O)_{z-1} + H_2O$.[35] For $z = 3$, the 0 K bond enthalpies calculated at the B3LYP, B3P86, and MP2(full) levels of theory are 86.1, 87.8, and 88.0 kJ/mol respectively, which are in close agreement with the experimentally determined value of 85.8 ± 5.4 kJ/mol. For $z = 2$, the calculated 0 K enthalpies are 143.8, 149.2, and 138.7 kJ/mol respectively, where the MP2(full) value is in best agreement with the experimental value of 135.6 ± 5.4 kJ/mol.

The ground states (GS) of the reactant zinc water complexes are taken from article 1,[1] which explored all possible low lying isomers of $Zn^{2+}(H_2O)_x(H_2O)_y$, where $x = 1-4$ and $y = 0$, $x = 4$ and $y = 1-6$, $x = 5$ and $y = 0-5$, and $x = 6$ and $y = 0-4$.

Results and Discussion

CID Cross Sections. Experimental cross sections for collision-induced dissociation of $Zn^{2+}(H_2O)_n$, where $n = 7 - 10$, with Xe are shown in parts a−d of Figure 1 and acquired as detailed in article 1.[1] In all cases, the loss of a single water molecule, reaction 1, is the dominant process, followed by loss of additional water molecules as the translational energy increases. There are three independent charge-separation processes that complicate the dissociation of $Zn^{2+}(H_2O)_6$, $Zn^{2+}(H_2O)_7$, and $Zn^{2+}(H_2O)_8$.

Part a of Figure 1 shows that the $Zn^{2+}(H_2O)_7$ complex dissociates by charge separation in reaction 5 at lower energies than the loss of a water molecule in reaction 1.

$$Zn^{2+}(H_2O)_7 + Xe \rightarrow ZnOH^+(H_2O)_3 + H^+(H_2O)_3 + Xe \quad (5)$$

However, despite having a lower apparent threshold, this process has a smaller cross section compared to that for water loss above about 0.4 eV. On the basis of the magnitudes of the two cross sections, charge separation is an entropically disfavored reaction by a factor of about 6 near 1 eV. This is consistent with the need to pass over the tight TS corresponding to the Coulombic barrier, whereas water loss involves a loose TS. The cross section for reaction 5 initially decreases with energy and then rises near 0.2 eV. This behavior indicates that reaction 5 is endothermic by less than reaction 1 and that there is sufficient internal energy available in the $Zn^{2+}(H_2O)_7$ reactant that a fraction of the complexes dissociate readily at very low collision energies. The magnitudes of the cross sections for the two charge-separated products should be identical but that for the protonated water cluster is smaller than for the hydrated zinc hydroxide, a result observed in most of the systems examined here and for other hydrated metal dications examined in our laboratory. These differences must be a result of lower collection

efficiency of the lighter product ion, which is particularly problematic in these systems because the charge-separation products have appreciable kinetic energies resulting from the Coulombic repulsion once they pass over the Coulomb barrier. Because the momentum of the two products must be equal, the lighter product has a higher energy by a factor corresponding to the mass ratio of the two products. This has been qualitatively confirmed for the charge separation of $Ca^{2+}(H_2O)_2$ by verifying that the ratio of the two singly charged products is sensitive to the focusing and transmission characteristics past the reaction region. (Of course, in our apparatus as well as all others, there is no guarantee that the collection of all products is 100% but the rf octopole surrounding the reaction region and the subsequent focusing optics have proven to efficiently transmit products in the majority of systems we have examined over several decades of experiments. The discussion here points out that the light ion in the charge-separation pair is particularly susceptible to losses because of its large kinetic energy release. Indeed, the transmission studies performed on the $Ca^{2+}(H_2O)_2$ system find that the magnitudes of the cross sections for water loss are invariant with focusing, those for the hydroxide ion product are affected slightly (by less than the 20% uncertainty in the absolute cross section magnitudes), whereas those for the hydrated hydronium ion products can change appreciably (factors of two). Indeed the ratio of the two products observed here is substantially closer to unity than in previously published work on analogous systems.[10,11])

In the dissociation of $Zn^{2+}(H_2O)_8$, the lowest-energy charge-separation process observed is reaction 6.

$$Zn^{2+}(H_2O)_8 + Xe \rightarrow ZnOH^+(H_2O)_4 + H^+(H_2O)_3 + Xe \quad (6)$$

Here, the cross sections for both ionic products agree in magnitude up to about 0.5 eV, as shown in part b of Figure 1. The apparent threshold for this reaction is higher in energy than the apparent threshold for simple water loss in reaction 1, a result that can also be observed in part c of Figure 1. The $ZnOH^+(H_2O)_4$ product was not collected for $Zn^{2+}(H_2O)_{10}$ (part d of Figure 1) because of its very low intensity, near the detection limit. The exothermic tail observed for the $ZnOH^+(H_2O)_4$ and $H^+(H_2O)_3$ product channels in part b of Figure 1 is a result of multiple collisions and disappears once these cross sections are extrapolated to zero pressure (below). Because reaction 6 is now both thermodynamically and entropically disfavored compared with reaction 1, the magnitude of its cross sections is less than 1% of the magnitude of that for reaction 1, much smaller than the relative magnitudes of the corresponding products in part a of Figure 1. Above about 0.5 eV, the $H^+(H_2O)_3$ cross section increases relative to the $ZnOH^+(H_2O)_4$ cross section, as shown in part b of Figure 1. This increase in the $H^+(H_2O)_3$ cross section matches the appearance of the $ZnOH^+(H_2O)_3$ product, indicating the onset of reaction 5, the charge-separation reaction from the primary $Zn^{2+}(H_2O)_7$ product, which is much more efficient than reaction 6. The relative thresholds for appearance of $Zn^{2+}(H_2O)_6$ and $ZnOH^+(H_2O)_3$ make it very clear that reaction 5 does indeed have a lower threshold than the water loss channel, consistent with our conclusions above from part a of Figure 1.

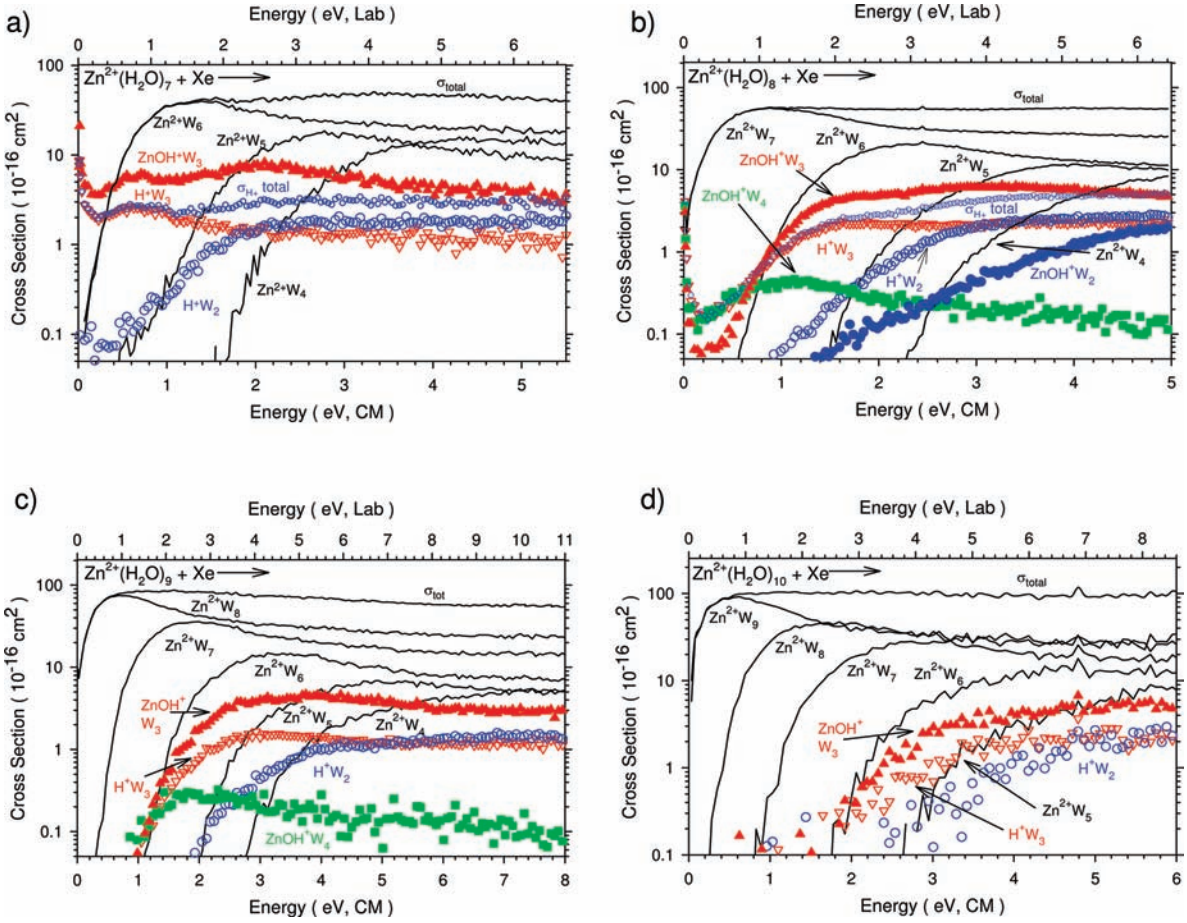

Figure 1. CID cross sections for the sequential water loss (lines) and charge-separation processes (symbols) for $Zn^{2+}W_n$ where $n = 7-10$ and W = H_2O (parts a–d respectively) colliding with Xe at 0.2 mTorr as a function of energy in the laboratory (upper x axis) and center of mass (lower x axis) frames. Hydrated zinc hydroxide ion products are shown by solid symbols and protonated water complex products by open symbols.

The cross sections of the $ZnOH^+(H_2O)_3$ product ions in both parts a and b of Figure 1 exhibit a second feature at higher energies beginning near 1 and 2 eV, respectively. This increase is not mirrored in the $H^+(H_2O)_3$ cross sections but is found in the sum of the $H^+(H_2O)_3$ and $H^+(H_2O)_2$ cross sections under all conditions and for all complex sizes. The appearance of these higher-energy features is much more obvious when the cross sections are viewed on a linear scale. Multiple experiments were conducted to see whether these features might be an artifact but no indications of this were found. Therefore, we conclude that this second feature is explained by the charge-separation process, reaction 7.

$$Zn^{2+}(H_2O)_6 \rightarrow ZnOH^+(H_2O)_3 + H^+(H_2O)_2 \qquad (7)$$

The apparent threshold of this charge-separation process is lower in energy than the water loss dissociation to form $Zn^{2+}(H_2O)_5$, as shown in parts a and b of Figure 1, such that the magnitudes of the charge-separated product cross sections are about 45% of that for water loss when comparing the respective maximum cross sections. Because both charge-separation processes 5 and 7 are energetically more favorable than the competing water loss reactions, the question of why smaller $Zn^{2+}(H_2O)_n$ complexes are seen in CID arises. These smaller clusters are formed because the sequential water loss channels are entropically favored. The density of states is much higher for the water loss channels because of the loose water loss TS compared to the tight TS needed for charge-separation. Because the threshold difference between the competing channels is relatively small, the water loss channels are still a dominant process in the dissociation behavior even though energetically more costly.

The cross section for $ZnOH^+(H_2O)_2$ is seen in part b of Figure 1 but because of the small intensity of this product it was not collected for the other reactant ions in parts a, c, and d of Figure 1. This cross section rises very slowly above about 1.0 eV, which makes it difficult to ascertain whether it originates from the charge-separation process, reaction 8,

$$Zn^{2+}(H_2O)_5 \rightarrow ZnOH^+(H_2O)_2 + H^+(H_2O)_2 \qquad (8)$$

or from the sequential loss of a water ligand from the $ZnOH^+(H_2O)_3$ product formed in reactions 6 and 7. This process is investigated further using theoretical calculations, as discussed below.

Charge-separation reactions observed in the dissociation of $Zn^{2+}(H_2O)_9$ and $Zn^{2+}(H_2O)_{10}$, parts c and d of Figure 1, mirror the results found for the smaller complexes. As noted above, the results of part c of Figure 1 clearly show that reaction 6 has a higher threshold energy than water loss from $Zn^{2+}(H_2O)_8$, whereas reaction 5 has a lower threshold energy than water loss from $Zn^{2+}(H_2O)_7$. In part d of Figure 1, only the most intense charge-separation products, those from reactions 5 and 7 are now observed.

Thermochemical Results. Cross sections for the primary and secondary dissociation products were analyzed using eq 3 in several ways, with Table 1 summarizing the average modeling parameters used. Threshold E_0 values are given for the primary dissociation of each complex from modeling with eq 3, which includes lifetime effects. If lifetime effects are not included, the threshold obtained from analysis is higher because of a kinetic shift. The kinetic shifts for the charge-separation reactions 5 and 6 are both about 0.1 eV. Those for the water loss products are discussed in article 1.[1]

The energy-dependent cross sections for the primary reaction pathways of $Zn^{2+}(H_2O)_8$ and $Zn^{2+}(H_2O)_7$ are influenced by the competition between the water loss and charge-separation processes. Modeling of these competitive reactions using eq 3 can also include the sequential dissociation of the primary product of the water loss channel, which then includes the effects of competition felt by the secondary water loss. Figure 2 shows a representative model of the competitive dissociation of $Zn^{2+}(H_2O)_8$ when analyzed as a $Zn^{2+}(H_2O)_5(H_2O)_3$ or (5,3) complex competitively dissociating to (4,3) + H_2O products and $ZnOH^+(H_2O)_4 + H^+(H_2O)_3$ or TS[4 + 3], where the primary (4,3) product ion sequentially dissociates to (4,2) + H_2O products. (At present, the computational machinery used for our data analysis, the CRUNCH program, is not capable of performing a competitive analysis of a sequential dissociation product, such as $Zn^{2+}(H_2O)_8 \rightarrow Zn^{2+}(H_2O)_7 + H_2O \rightarrow Zn^{2+}(H_2O)_6 + 2H_2O$ competing with $Zn^{2+}(H_2O)_8 \rightarrow Zn^{2+}(H_2O)_7 + H_2O \rightarrow ZnOH^+(H_2O)_3 + H^+(H_2O)_3$.) To determine the competitive shift, the threshold values obtained in this work are compared to the values where competition is not accounted for, as reported in article 1.[1] In the competitive analyses, it is found that whichever process has the lower-energy threshold is essentially unaffected by the competition regardless if the TS is loose (water loss) or tight (charge separation). Thus, reaction 1 for $Zn^{2+}(H_2O)_8$ has a threshold of 0.71−0.76 eV when modeled as a (5,3) → (4,3) + H_2O dissociation no matter if the cross section is fit independently or with competition, whereas the higher-energy charge-separation channel shows a competitive shift of 0.14−0.16 eV. In contrast, analysis of $Zn^{2+}(H_2O)_7$ dissociation (when modeled as (4,3) → (4,2) + H_2O → (4,1) + $2H_2O$ competing with (4,3) → TS[3 + 3]) finds that the lower-energy charge-separation channel has a threshold of 0.69 eV for all modeling conditions, whereas the threshold for reaction 1 shifts down by about 0.06 eV when competition is included (and that for the secondary water loss channel shifts down by 0.18 eV).

As noted in article 1,[1] theory yields ambiguous results regarding the GS of the $Zn^{2+}(H_2O)_n$ complexes. Because a distribution of reactant and product GS isomers may be possible, the water loss dissociation pathways were analyzed with several assumed dissociation pathways (as described in detail in article 1). Depending on the isomers chosen in the data analysis, the kinetic shift may change slightly leading to a change in the E_0 threshold for dissociation. Although the structures of the calculated charge separation tight TSs do not depend on the reactant isomer, the reactant isomer chosen for data analysis will affect the kinetic shift. As previously discussed in article 1, complexes like (4,4), (4,3), and (4,3)_2D,DD_AA,2A have larger densities of states than their counterparts with more inner-shell water molecules because the additional outer-shell waters have lower torsional frequencies. Thus, these reactants increase the time for dissociation, which increases the kinetic shift (lowering E_0) compared to the more constrained 5- and 6-inner-shell coordinate complexes. Although the E_0 values change according to the kinetic shift, the competitive shift between modeling with and without including competition remains fairly constant regardless of the reactant isomer. The charge-separation process for the $Zn^{2+}(H_2O)_8$ complex has a competitive shift of 0.14−0.19 eV, whereas the water loss threshold remains constant within experimental uncertainty with or without including competition, for all isomers. Likewise, the competitive shifts for the primary and secondary water loss dissociations

TABLE 1: Optimized Parameters from Analysis of CID Cross Sections for $Zn^{2+}(H_2O)_{7,8}$[a]

reactant	product	σ_0	N	E_0 (eV)	$\Delta S^{\ddagger}_{1000\ K}$ J/(mol K)
(5,3)	(4,3)[b,c]	67 (6)	0.8 (0.2)	0.71 (0.07)	65 (8)
	TS[4 + 3][b]	0.52 (0.2)	0.6 (0.2)	0.94 (0.07)	96 (5)
	(4,3)[b,c]	68 (5)	0.8 (0.2)	0.72 (0.06)	67 (9)
	(4,2)[b,c]	48 (5)	0.8 (0.2)	1.68 (0.06)	96 (5)
	(4,3)[d]	76 (4)	0.8 (0.2)	0.73 (0.06)	65 (10)
	TS[4 + 3][d]	0.03 (0.01)	0.8 (0.2)	**0.80 (0.05)**	96 (5)
	(4,3)[e]	75 (3)	0.7 (0.1)	0.76 (0.04)	68 (9)
	(4,2)[e]	59 (9)	0.7 (0.1)	1.75 (0.05)	
	TS[4 + 3][e]	0.010 (0.003)	0.7 (0.1)	**0.78 (0.05)**	96 (5)
(5,3)	(5,2)[b,c]	66 (6)	0.8 (0.2)	0.68 (0.07)	55 (8)
	(5,2)[d]	75 (4)	0.8 (0.2)	0.70 (0.06)	54 (10)
	TS[4 + 3][d]	0.01 (0.01)	0.8 (0.2)	**0.77 (0.05)**	96 (5)
(4,4)	(5,2)[b,c]	65 (6)	0.8 (0.2)	0.62 (0.07)	17 (8)
	TS[4 + 3][b]	0.5 (0.2)	0.7 (0.2)	0.88 (0.07)	53 (5)
	(5,2)[d]	73 (4)	0.9 (0.2)	0.62 (0.06)	18 (10)
	TS[4 + 3][d]	0.01 (0.01)	0.9 (0.2)	**0.69 (0.05)**	53 (5)
(4,4)	(4,3)[b,c]	66 (6)	0.8 (0.2)	0.66 (0.07)	22 (8)
	(4,3)[d]	76 (4)	0.9 (0.2)	0.66 (0.06)	65 (10)
	TS[4 + 3][d]	0.03 (0.01)	0.9 (0.2)	**0.73 (0.05)**	53 (5)
(4,3)	(4,2)[b,c]	58 (5)	0.7 (0.2)	0.89 (0.06)	18 (7)
	TS[3 + 3][b]	7 (1)	0.9 (0.2)	0.69 (0.05)	110 (5)
	(4,2)[b,c]	58 (7)	0.8 (0.2)	0.88 (0.07)	19 (10)
	(4,1)[b,c]	37 (10)	0.8 (0.2)	2.02 (0.09)	
	(4,2)[d]	63 (6)	0.9 (0.3)	**0.81 (0.05)**	17 (7)
	TS[3 + 3][d]	7×10^{-6} (5×10^{-6})	0.9 (0.3)	0.69 (0.06)	110 (5)
	(4,2)[e]	67 (4)	0.9 (0.1)	**0.82 (0.05)**	17 (9)
	(4,1)[e]	21 (12)	0.9 (0.1)	**1.84 (0.08)**	
	TS[3 + 3][e]	4×10^{-6} (3×10^{-6})	0.9 (0.1)	0.69 (0.05)	110 (5)
(4,3)_2D,DD_AA,2A	(4,2)[b,c]	58 (5)	0.7 (0.2)	0.81 (0.06)	−29 (7)
	TS[3 + 3][b]	7 (1)	0.9 (0.2)	0.66 (0.06)	62 (5)
	(4,2)[d]	61 (6)	0.9 (0.3)	**0.74 (0.05)**	−29 (7)
	TS[3 + 3][d]	7×10^{-6} (5×10^{-6})	0.9 (0.3)	0.66 (0.06)	62 (5)
(5,2)	(6,0)[b,c]	58 (7)	0.8 (0.2)	0.90 (0.07)	63 (10)
	(5,0)[b,c]	37 (10)	0.8 (0.2)	2.00 (0.09)	
	TS[3 + 3][b]	7 (1)	0.9 (0.2)	0.70 (0.05)	115 (5)
	(6,0)[e]	65 (4)	1.0 (0.1)	**0.82 (0.05)**	61 (9)
	(5,0)[e]	22 (12)	1.0 (0.1)	**1.80 (0.08)**	
	TS[3 + 3][e]	6×10^{-6} (3×10^{-6})	1.0 (0.1)	0.69 (0.05)	115 (5)
(5,2)	(5,1)[b,c]	58 (7)	0.8 (0.2)	0.95 (0.07)	76 (10)
	(5,0)[b,c]	37 (10)	0.8 (0.2)	1.98 (0.09)	
	(5,1)[e]	65 (4)	1.0 (0.1)	**0.85 (0.05)**	74 (9)
	(5,0)[e]	20 (12)	1.0 (0.1)	**1.79 (0.08)**	
	TS[3 + 3][e]	9×10^{-6} (3×10^{-6})	1.0 (0.1)	0.73 (0.05)	115 (5)

[a] Uncertainties in parentheses. Values in bold provide the best values and highlight threshold energies that differ from less sophisticated modeling. [b] No competition included. [c] Values reported in article 1.[1] [d] Competitive dissociation modeling using eq 3. [e] Competitive and sequential dissociation modeling using eq 3.

for the $Zn^{2+}(H_2O)_7$ complexes are 0.06−0.10 eV and 0.18−0.20 eV, respectively.

As noted above, vibrational frequencies and rotational constants for the loose TSs associated with water loss were taken directly from the theoretical calculations in article 1. Those for the tight charge-separation TSs are calculated as described below. In each of these TSs, the lowest vibrational frequency (~4 cm^{-1}) corresponds to a torsion of the complex about the reaction coordinate. The next four vibrations (8−63 cm^{-1}) correspond to hindered rotations of the incipient $ZnOH^+(H_2O)_m$ and $H^+(H_2O)_{n-m-1}$ products at the TS. These five vibrations were treated as rotational degrees of freedom during the analysis. This treatment gave models that reproduced the energy dependence of the experimental cross sections but also made this TS looser, greatly decreasing the scaling factor, $\sigma_{0,j}$ needed in the competitive and competitive sequential fits (Table 1). Treatment of these five degrees of freedom as vibrations yielded scaling factors ($\sigma_{0,j}$) closer to unity, but the energy dependences were not described as accurately because the model deviates strongly from the data at higher energies, as shown in Figure S1 of the Supporting Information. The charge-separation E_0 decreases because the product has fewer rotational degrees of freedom, which reduces the number of states at the transition state, thereby increasing the kinetic shift.

Theoretical Results. Theoretical geometries and relative energetics of $Zn^{2+}(H_2O)_n$, where $n = 1-10$, for multiple isomers with inner solvent shell sizes of 4, 5, and 6 are presented in article 1.[1] Given the ground state structures of the zinc dication water complexes, the mechanism for the charge-separation processes can be seen to be complex. For instance, formation of $ZnOH^+(H_2O)_3 + H^+(H_2O)_3$ from $Zn^{2+}(H_2O)_7$ requires that two of the outer-shell waters in the (4,3)_2AA,A structure must move to create a third solvent shell (4,1,2)_AADD_2A, thus forming the $H^+(H_2O)_3$ leaving group. To investigate this charge-separation process more thoroughly, a complete reaction coordinate path for this dissociation was investigated theoretically. As mentioned above, the path was first generated by scanning along the likely reaction coordinates at a B3LYP/6-31G(d) level, with the geometries and energies of the TSs and intermediates (INTs) further optimized at the B3LYP/6-

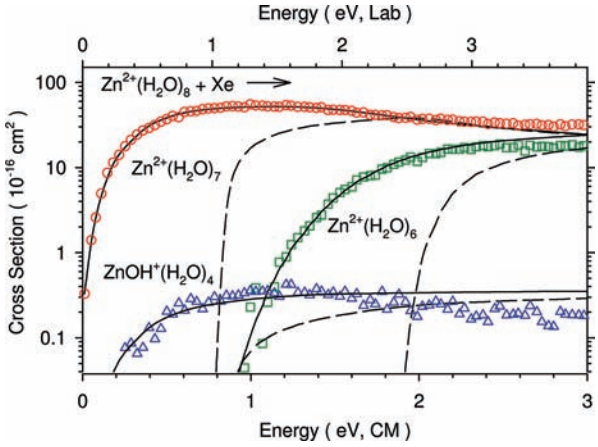

Figure 2. Zero pressure extrapolated cross sections for the CID of $Zn^{2+}(H_2O)_8$ with Xe. Solid lines show the best fit to both the primary and secondary water loss and the competing charge-separation product ion using eq 3 convoluted over the kinetic and internal energy distributions of the neutral and ionic reactants. Dashed lines show the models in the absence of experimental kinetic energy broadening for reactants with an internal energy of 0 K. Optimized parameters for this fit are found in Table 1.

311+G(2d,2p)//B3LYP/6-311+G(d,p) level. The surface generated describes the proton transfer mechanism and is shown in Figure 3 with energies listed in Table 2. In this mechanism, the singly bound second-shell water ligand of the (4,3)_2AA,A GS moves forming TS1, 29.4 kJ/mol higher in energy, as it bridges between an inner and a second solvent shell water. INT1, (4,2,1)_AA,AAD_A, is then formed as this water molecule enters the third solvent shell. A more complex path is required to move the next water molecule, which is doubly hydrogen bonded in the second shell of the (4,3) GS and INT1. One of those hydrogen bonds must first be broken and then the water can move closer to the leaving group creating a series of shallow TSs and INTs. In TS5, 53.9 kJ/mol above the (4,3) GS and 30.0 kJ/mol above INT4, (4,2,1)_AAD,A_A, this water bridges the first and second solvent shell, explaining the similarity in energy relative to the 29.4 kJ/mol difference between TS1 and the (4,3) GS. Finally, the rate-limiting step is TS7 = TS[3 + 3], 70.7 kJ/mol above the (4,3) GS, where the $H^+(H_2O)_3$ pulls away leaving $ZnOH^+(H_2O)_3$, which has a pseudotetrahedral geometry. Overall, this charge-separation process is calculated to be exothermic by 68.9 kJ/mol at this level of theory, as shown in Table 2.

Complete reaction coordinates for the $n = 5$, 6, and 8 charge separations were not fully optimized but must follow a similar pathway for proton transfer as the $n = 7$ charge separation. In all these cases, it is clear that the rate-limiting step needed for thermochemical analysis is the TS with $H^+(H_2O)_{n-m-1}$ pulling away from $ZnOH^+(H_2O)_m$, where $m = 2$ for $n = 5$, $m = 3$ for $n = 6$, and $m = 4$ for $n = 8$. The optimized tight TSs of the charge-separation processes occurring for $n = 5$, 6, and 8 are shown in Figure 4. The structure of the $ZnOH^+(H_2O)_4$ complex is the GS at all three levels of theory and has the fourth water in the second shell forming three hydrogen bonds, one donor bond with the hydroxide group, and two acceptor bonds with inner-shell water molecules. Although $ZnOH^+(H_2O)_4$ has an overall single charge, its structure once again demonstrates the ability of the zinc dication to form stable structures at an inner-shell size of four. A five coordinate $ZnOH^+(H_2O)_4$ was also investigated, where the inner shell forms a square pyramidal shape with the hydroxide group bonding to the Zn^{2+} at the base of the square pyramid. This is found to be higher in energy by 20−27 kJ/mol at all three levels of theory.

Energies for the rate-limiting TSs for $n = 5$, 6, and 8 are listed in Table 2 along with the respective exothermicities of the overall charge-separation processes. Relative to the ground-state reactant complexes, the energetic barriers for $n = 5-7$ are within 5 kJ/mol of each other (72.6, 74.6, and 70.7 kJ/mol, respectively), whereas that for $n = 8$ is higher at 99.4 kJ/mol. (Similar trends are found for both B3P86 and MP2(full) calculations, with B3P86 energies being very similar to the B3LYP energies and those for MP2(full) being 5−23 kJ/mol higher, Table 3.) This large change in the barrier may be explained by differences between the structure of the hydroxide complexes at the TS and in the GS products. The $ZnOH^+(H_2O)_2$ and $ZnOH^+(H_2O)_3$ moieties in the $n = 5-7$ TSs are structurally close to their respective GS products, as shown in Figures 3, 4, and Figure S2 of the Supporting Information, thereby minimizing the energy of the TS. However, the additional water ligand in the $ZnOH^+(H_2O)_4$ complex is involved in three H-bonds as described above to stabilize the hydroxide group. Compared to the GS complex, each H-bond is much longer in TS[4 + 3], thereby increasing its energy. It can also be seen that the overall exothermicity of the charge-separation processes roughly increases as n decreases: 77.4, 65.7, 68.9, and 56.3 kJ/mol for $n = 5 - 8$ respectively such that the reverse Coulombic barrier increases as n decreases for $n = 5-7$: 150.0, 140.3, 139.6 kJ/mol, respectively. One potential reason for this increase is that as the complex gets smaller the dissociation is more like a pure electrostatic Coulomb repulsion. For example, in the charge separation of the $Zn^{2+}(H_2O)_5$ complex, there are fewer waters interacting with the two charge carriers in the TS and products, as shown in Figure 4 and in Figure S2 of the Supporting Information, respectively. This trend changes in moving from $n = 7$ to 8 as the reverse Coulombic barrier is highest for $n = 8$, 155.7 kJ/mol, as rationalized by the structural changes in the hydroxide needed to form three H-bonds, as described above.

Experimental Transition-State Energies and Comparison to Theory. Article 1 contains a detailed examination of the comparison between experimental and theoretical 0 K hydration energies. Excellent agreement with theory is found for $n = 6-8$, which verifies the importance of including the competitive shifts. Table 3 compares the experimental dissociation 0 K thresholds for charge separation, which include competitive shifts, to the values predicted by theory for these rate-limiting TSs. There is good agreement for all three reactant isomers at $n = 7$, although the MP2 values are somewhat high (by 12 − 27 kJ/mol). However, theory predicts an energy for the charge-separation TS of the $n = 8$ complex that is 34−44 kJ/mol above the experimental value for both the (5,3) and (4,4) reactants. As discussed in article 1,[1] this is a further indication that there is a need for additional experimental and theoretical work at cluster sizes of $n \geq 8$.

In addition, Table 3 also compares both the experimental thresholds and theoretically predicted 0 K enthalpies required for charge separation versus water loss. Although no experimental dissociation energies are available for $n = 5$ as of yet, theory favors charge separation over water loss by 28−30 kJ/mol at the DFT levels and 9 kJ/mol at the MP2(full) level, in qualitative agreement with our observations for reaction 8. Likewise, for $n = 6$, theory predicts charge separation is favored by about 22−25 kJ/mol (DFT) or 9 kJ/mol (MP2), as clearly observed experimentally for reaction 7. For a four coordinate $n = 7$ reactant, DFT predicts that the charge-separation reaction 5 is favored by 9−10 kJ/mol, whereas MP2(full) finds that the water loss channel is favored by about 6 kJ/mol. For the (5,2) complex, DFT favors charge separation by 23−25 kJ/mol;

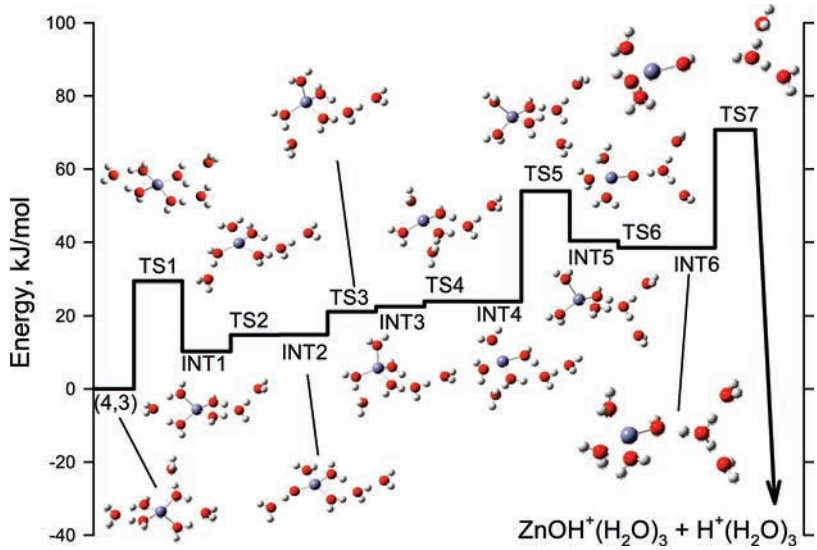

Figure 3. Complete reaction coordinate for $Zn^{2+}(H_2O)_7$ charge separating to $ZnOH^+(H_2O)_3 + H^+(H_2O)_3$ calculated at a B3LYP/6-311+G(2d,2p)//B3LYP/6-311+G(d,p) level of theory including zero point energy corrections. Optimized structures of the transition states (TS) are shown above the surface and intermediates (INT) are below.

TABLE 2: Relative Energies (kJ/mol) for Intermediates (INT) and Transition States (TS) Along the Reaction Coordinate for Charge Separation of $Zn^{2+}(H_2O)_{5-8}$ Calculated at the B3LYP/6-311+G(2d,2p)//B3LYP/6-311+G(d,p) Level

species	relative energy
$Zn^{2+}(H_2O)_5$ (4,1)	0.0
TS [2 + 2]	72.6
$ZnOH^+(H_2O)_2 + H^+(H_2O)_2$	−77.4
$Zn^{2+}(H_2O)_6$	0.0
TS [3 + 2]	74.6
$ZnOH^+(H_2O)_3 + H^+(H_2O)_2$	−65.7
$Zn^{2+}(H_2O)_7$ (4,3)	0.0
TS1	29.4
INT1	10.3
TS2	14.8
INT2	14.9
TS3	21.1
INT3	22.5
TS4	24.0
INT4	23.9
TS5	53.9
INT5	40.3
TS6	38.5
INT6	38.4
TS7 = TS[3 + 3]	70.7
$ZnOH^+(H_2O)_3 + H^+(H_2O)_3$	−68.9
$Zn^{2+}(H_2O)_8$ (5,3)	0.0
TS [4 + 3]	99.4
$ZnOH^+(H_2O)_4 + H^+(H_2O)_3$	−56.3

however, MP2(full) again predicts that water loss is preferred, by 11 kJ/mol. The experimental results definitively show that charge separation is favored, with an average energy difference determined from competitive modeling of 11 ± 2 kJ/mol. Finally, for $n = 8$, experiment and theory agree that water loss is favored over the charge-separation reaction 6, with an average threshold difference of 5 ± 2 kJ/mol, compared to the DFT prediction of about 19−23 kJ/mol and 30 − 42 kJ/mol for MP2(full). Clearly, the MP2(full)//B3LYP calculations are overestimating the energy barrier for charge separation. Because of this discrepancy, MP2(full) geometry optimizations were performed on these TSs. Energies calculated at the MP2//MP2 level are 5 kJ/mol lower for the (4,1) GS and 3 kJ/mol higher for TS[2 + 2] than the MP2//B3LYP energies. Accordingly,

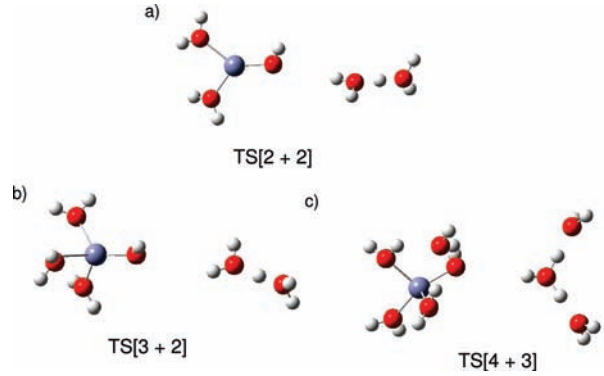

Figure 4. Optimized rate-limiting transition states of the $n = 5$, 6, and 8 charge-separation products $ZnOH^+(H_2O)_m + H^+(H_2O)_{n-m-1}$, where $m = 2$, 3, and 4 and $n - m - 1 = 2$, 2, and 3 for parts a−c respectively calculated at the B3LYP/6-311+G(d,p) level of theory.

the MP2//MP2 predicted barrier for the $n = 5$ charge separation is 8 kJ/mol higher in energy than the MP2//B3LYP barrier. Thus, this more computationally expensive procedure does not appear to give a better estimation for these charge-separation barriers.

Using Coulomb's law to calculate the reverse barrier from the charge-separation products to their TS, we find that the barriers are similar for all complex sizes, ranging from 188−210 kJ/mol, because the product separation at the TS (chosen as the separation between the two center of masses of each charged species) varies little, 6.58−7.35 Å. These electrostatic barriers are much higher in energy than the TS values given by either modeling the experimental results or the computed reaction coordinate but the electrostatic barriers do not account for any covalent interactions between the two charged products at the optimized separation distance nor for any delocalization of the charge resulting from hydration.

Using the calculated frequencies and rotational constants of the tight transition states for charge separation, a rigid rotor/harmonic oscillator approximation was applied to convert the 0 K barrier heights of the $n = 7$ and 8 reactants to 298 K values in Table 4. The (4,3) and (5,3) reactants are selected as representative of these complexes. The uncertainties in these conversions are found by scaling the vibrational frequencies up and down by 10%. Because the conversion to 298 K depends

TABLE 3: Comparison of 0 K Transition-State Energies to Theory (kJ/mol)

n	reactant	product	experiment	B3LYP[a]	B3P86[a]	MP2(full)[a]
5	(4,1)	TS[2 + 2]		72.6	74.3	90.1
		(4,0)		100.3	104.1	98.6
6	(4,2)	TS[3 + 2]		74.6	75.5	86.6
	(4,2)	(4,1)	98.4 (3.9)[b]	97.0	100.6	95.7
7	(4,3)	TS[3 + 3]	66.6 (5.8)[c]	70.7	72.2	82.9
		(4,2)	78.2 (4.8)[b]	79.8	82.5	76.5
	(4,3)_2D,DD AA,2A	TS[3 + 3]	63.7 (5.8)[c]	66.6	68.1	75.8
		(4,2)	71.4 (4.8)[b]	75.7	78.4	69.3
	(5,2)	TS[3 + 3]	66.6 (4.8)[c]	70.6	72.1	93.8
		(6,0)	79.2 (4.8)[b]	93.5	97.0	83.3
8	(4,4)	TS[4 + 3]	68.5 (6.8)[c,d]	97.7	95.6	102.9
		(4,3)	63.7 (5.8)[b]	74.8	77.0	72.7
	(5,3)	TS[4 + 3]	74.3 (4.8)[c]	99.4	98.0	117.8
		(5,2)	68.5 (10.5)[b,d]	76.0	78.8	75.4

[a] Geometry optimizations calculated using B3LYP/6-311+G(d,p) and SPE values calculated with a 6-311+G(2d,2p) basis set at the level indicated. All values are ZPE corrected. [b] Values reported in article 1.[1] [c] Values taken from Table 1 using competitive modeling with eq 3. [d] Average of primary and secondary thresholds reported in article 1.[1]

TABLE 4: Conversion of 0 K Thresholds to 298 K Enthalpies and Free Energies for the Charge-Separation Transition States for $Zn^{2+}(H_2O)_{7,8}$; All Values in kJ/mol with Uncertainties in Parentheses

complex	ΔH_0[a]	$\Delta H_{298} - \Delta H_0$[b]	ΔH_{298}	$T\Delta S_{298}$	ΔG_{298}
TS[3 + 3]	66.6 (5.8)	1.6 (0.1)[c]	68.2 (5.8)	41.6 (1.0)[c]	26.6 (5.9)
		7.0 (0.2)[d]	73.6 (5.8)	24.8 (1.0)[d]	48.8 (5.9)
TS[4 + 3]	74.3 (4.8)	−0.6 (0.4)[c]	73.7 (4.8)	39.5 (1.1)[c]	34.2 (4.9)
		4.6 (0.3)[d]	78.9 (4.8)	16.4 (1.0)[d]	62.5 (4.8)

[a] Experimental values from Table 3. [b] Values calculated from the vibrations and rotations calculated at the B3LYP/6-311+G(d,p) level. Uncertainties found by scaling the frequencies up and down by 10%. [c] Values calculated with the first 5 vibrations of the TS being treated as rotations. [d] Values calculated using all vibrations.

on the vibrations and rotations of the complex, there are two possible conversion values for the charge-separation TSs depending on whether the five low-frequency torsions are treated as vibrations or rotors. When treated as rotors, the 298 K enthalpies for the charge-separation TSs at $n = 7$ and 8 are 68.2 and 73.7 kJ/mol respectively but rise to 73.6 and 78.9 kJ/mol respectively when vibrations are used for the low-frequency torsions. Thus, the conversion values of the two different methods differ from each other by about 5 kJ/mol. The entropies of dissociation, $T\Delta S_{298}$, for the charge-separation TSs are larger when the first five vibrations of the TS are treated as rotations because of the larger rotational entropy of the product. Thus, the ΔG_{298} values are smaller for the charge-separation TSs when the first five vibrations of the TS are treated as rotations compared to results when all vibrations are used in the TS. Without a more thorough analysis of the potential energy surfaces involved, it is difficult to state with certainty whether the treatment of these degrees of freedom as vibrations or rotations is more correct. We are inclined to believe they should be treated as rotations and note that this model fits the charge-separation data better at higher energies, as noted above.

Critical Size. Previous studies have defined the critical size as the value of *n* where "the charge reduction reaction...becomes competitive with single ligand loss"[11] and equivalently as "the maximum number of ligands at which dissociative charge transfer is competitive with simple ligand loss."[10] Such a definition is an empirical one that is highly dependent on instrumental sensitivity and product collection (which is more difficult for the charge-separation products because of the kinetic energy release). Furthermore, previous studies of the critical size have relied primarily on observations of the maximum size of the hydroxide ion products. Indeed, Blades et al.[11] assign all their critical sizes as the value of $m + 2$ in reaction 2, on the basis that the only protonated water cluster they observed with any intensity was H_3O^+. Thus, they assigned $n_{crit} = 5$ for Zn^{2+} because the largest hydroxide complex they observed was $ZnOH^+(H_2O)_3$. Shvartsburg and Siu[10] also use their observation of "the largest singly charged hydrated metal ions" as the basis for assigning their critical values, but often get values larger by 1 compared to Blades et al., for example, $n_{crit} = 6$ for Zn^{2+}. They suggest this is because their higher sensitivity allows them to see complexes corresponding to larger values of *m* and $n-m-1$. Notably, Shvartsburg and Siu also point out, quite correctly, that the n_{crit} values could be lower limits if for instance the hydrated metal hydroxide cation complexes partially dissociate before observation. They also point out that tandem mass spectrometry experiments are required, otherwise the largest hydrated metal hydroxide cation observed could be generated in the source by hydration of smaller complexes.

Ultimately, both of these previous studies focus on the observation of the product ion rather than the behavior of the reactant ion, which is what the definition of critical size is supposed to specify. Thus, any study that does not allow some means of identifying which $MOH^+(H_2O)_m$ product is formed simultaneously with which $H^+(H_2O)_{n-m-1}$ product will fail to identify the correct precursor *n* that undergoes the charge-separation reaction 2. Thus, we observe that the $ZnOH^+(H_2O)_3$ complex is formed in greatest abundance, in agreement with the observations of Blades et al. who assign $n_{crit} = 5$. With greater sensitivity, however, the largest hydrated zinc hydroxide cation complex we observe is $ZnOH^+(H_2O)_4$, which, if formed along with H_3O^+, would lead to assignment of $n_{crit} = 6$, in agreement with Shvartsburg and Siu. However, the kinetic-energy resolved studies performed here clearly show that the latter hydroxide complex is accompanied by the $H^+(H_2O)_3$ product ion, and therefore comes from dissociation of the $Zn^{2+}(H_2O)_8$ complex, which would lead to the assignment $n_{crit} = 8$. Fundamentally, the key observations in all three studies are essentially the same but the final results differ because of instrumental sensitivity and the ability to assign the true products of the charge-separation reaction. Indeed, we find that three complexes of zinc definitely undergo charge separation, $n = 6-8$, and possibly 5, which according to a definition for n_{crit} that relies on the competitiveness of the charge reduction reaction with single ligand loss means that all three (possibly

four) complexes have the critical size. Clearly, there is no singular critical size that differentiates when charge separation is observed and when it is not.

If a singular (truly critical) value for n_{crit} is needed, then the observations of the present study dictate the need for a different definition for the charge-separation critical size. As noted above, the calculated barrier for charge separation for the $n = 5-7$ complexes remains fairly constant, whereas the hydration energies increase as the cluster gets smaller (article 1).[1] These trends demonstrate that there should be a maximum-sized cluster for which charge separation is energetically favored over the loss of one water ligand. We suggest that the critical size be equated with this size complex, which makes the definition of the critical size a thermodynamic one that depends solely on the relative energies of the barrier for charge separation versus that for loss of a water ligand. In general, for clusters larger than this critical size, charge separation is both energetically and entropically disfavored, such that this channel will be small (such as for $n = 8$ here) if observed at all. Note that the identification of n_{crit} as being less than 8 is verified by examination of the relative onsets of the products part b of in Figure 1, where the $ZnOH^+(H_2O)_4$ cross section has a apparent threshold that is clearly higher in energy than the competing water loss product forming $Zn^{2+}(H_2O)_7$. At the critical size, the favorable energy for charge separation will generally allow it to be observed experimentally unless entropy effects disfavoring it are substantial. Because of these features, this proposed definition will often coincide with the previous experimental definition although the correct assignment of n_{crit} still relies on the sensitivity of the apparatus and the correlation between the protonated hydrate and hydrated metal hydroxide cation complexes formed in reaction 2. (A reviewer also wonders whether tunneling through the charge-separation barrier might enhance the probability of observing charge separation even below its classical threshold energy. We believe this is unlikely to be influential given that our calculations indicate that the rate-limiting step for charge separation involves movements of the separating singly charged products away from one another. All proton motions susceptible to tunneling effects come before the rate-limiting step.) Using the presently proposed definition, the critical size for zinc hydration is $n_{crit} = 7$ as confirmed by both experimental thresholds and theoretical results. Consistent with these more quantitative evaluations, examination of part a of Figure 1 clearly shows that the $ZnOH^+(H_2O)_3 + H^+(H_2O)_3$ products have apparent thresholds that are lower in energy than the threshold for the competing water loss forming $Zn^{2+}(H_2O)_6$. Thus, thermal ion sources (such as our ESI source) will ordinarily be unable to generate hydrated complexes smaller than n_{crit} because charge separation will occur instead of evaporation of additional ligands. As shown in analogous studies on Cu^{2+} hydration, such small complexes can be formed by utilizing either high-energy collisional-activated dissociation (CAD),[36] which takes advantage of the entropic favorability of the dehydration reactions compared to charge separation, or a pickup technique,[37] in which water molecules are condensed onto a beam of neutral copper atoms and then ionized using electron ionization.

Conclusions

Collision-induced dissociation cross sections for $Zn^{2+}(H_2O)_n$, where $n = 7-10$, are examined in detail with regard to the charge-separation products, $ZnOH^+(H_2O)_m + H^+(H_2O)_{n-m-1}$. The experimental cross sections show that charge separation occurs at $n = 6-8$ and possibly at $n = 5$, although the latter products might also be the result of sequential dissociation. Because a range of complex sizes are observed to undergo charge separation in competition with dehydration, the critical size for charge separation is redefined as the largest value of n at which the charge separation is energetically favored over the loss of one water ligand. For $Zn^{2+}(H_2O)_n$ complexes, this means that $n_{crit} = 7$.

A complete reaction coordinate for the charge-separation dissociation at $n = 7$ is calculated and rate-limiting transition states for $n = 5$, 6, and 8 are also evaluated. The molecular parameters for these TSs are used to analyze the cross sections for collision-induced dissociation of $Zn^{2+}(H_2O)_7$ and $Zn^{2+}(H_2O)_8$ including the competition between dehydration and charge-separation reactions. As evaluated in article 1,[1] accounting for this competition is necessary for obtaining accurate hydration energies for $n = 6-8$. Although no experimental measurements are possible at this time for smaller complexes, theory indicates that the charge-separation process at $n = 5$ and 6 is favored over water loss. Because the Coulomb barrier for the charge-separation processes at $n = 5-7$ relative to the GS reactants are similar in energy, trends in the hydration energies indicate that the charge-separation process should be energetically favored for all $Zn^{2+}(H_2O)_n$ complexes when $n \leq n_{crit}$. As a consequence, formation of these smaller complexes in an ESI source will generally be limited and methods seeking to form them by dissociation should fail.

Acknowledgment. This work is supported by the National Science Foundation, Grant No. CHE-0748790. In addition, we thank the Center for High Performance Computing at the University of Utah for the generous allocation of computer time.

Supporting Information Available: Analysis of the CID cross sections of $Zn^{2+}(H_2O)_8$ when five degrees of freedom are treated as vibrations. Optimized GSs of the $n = 5$ and 8 charge-separation products, $ZnOH^+(H_2O)_m + H^+(H_2O)_{n-m-1}$, calculated at the B3LYP/6-311+G(d,p) level of theory. This material is available free of charge via the Internet at http://pubs.acs.org.

References and Notes

(1) Cooper, T.; Carl, D.; Armentrout, P. B. DOI: 10.1021/jp906235y.
(2) Spiro, T. G. *Zinc Enzymes*; J. Wiley: New York, 1983.
(3) Kimura, E. *Pure Appl. Chem.* **1993**, *65*, 355.
(4) Richens, D. T. *The Chemistry of Aqua Ions*; John Wiley and Sons, Inc: New York, 1997.
(5) Nriagu, J. O. *Zinc in the Environment*; Wiley: New York, 1980.
(6) Rudolph, W. W.; Pye, C. C. *Phys. Chem. Chem. Phys.* **1999**, *1*, 4583.
(7) Peschke, M.; Blades, A. T.; Kebarle, P. *Int. J. Mass Spectrom.* **1999**, *187*, 685.
(8) Peschke, M.; Blades, A. T.; Kebarle, P. *J. Am. Chem. Soc.* **2000**, *122*, 1492.
(9) Peschke, M.; Blades, A. T.; Kebarle, P. *J. Am. Chem. Soc.* **2000**, *122*, 10440.
(10) Shvartsburg, A. A.; Siu, K. W. M. *J. Am. Chem. Soc.* **2001**, *123*, 10071.
(11) Blades, A. T.; Jayaweera, P.; Ikonomou, M. G.; Kebarle, P. *Int. J. Mass Spectrom. Ion Processes* **1990**, *102*, 251.
(12) Chillemi, G.; D'Angelo, P.; Pavel, N. V.; Sanna, N.; Barone, V. *J. Am. Chem. Soc.* **2002**, *124*, 1968.
(13) D'Angelo, P.; Barone, V.; Chillemi, G.; Sanna, N.; Meyer-Klaucke, W.; Pavel, N. V. *J. Am. Chem. Soc.* **2002**, *124*, 1958.
(14) Pappalardo, R. R.; Marcos, E. S. *J. Phys. Chem.* **1993**, *97*, 4500.
(15) Bock, C. W.; Katz, A. K.; Glusker, J. P. *J. Am. Chem. Soc.* **1994**, *117*, 3754.
(16) Hartmann, M.; Clark, T.; vanEldik, R. *J. Mol. Model.* **1996**, *2*, 354.
(17) Lee, S.; Kim, J.; Park, J. K.; Kim, K. S. *J. Phys. Chem.* **1996**, *100*, 14329.
(18) Hartmann, M.; Clark, T.; vanEldik, R. *J. Am. Chem. Soc.* **1997**, *119*, 7843.

(19) Pavlov, M.; Siegbahn, P. E. M.; Sandstrom, M. *J. Phys. Chem. A* **1998**, *102*, 219.
(20) Rodgers, M. T.; Armentrout, P. B. *J. Chem. Phys.* **1998**, *109*, 1787.
(21) Muntean, F.; Armentrout, P. B. *J. Chem. Phys.* **2001**, *115*, 1213.
(22) Gilbert, R. G. Smith, S. C. *Theory of Unimolecular and Recombination Reactions*; Blackwell Scientific: Oxford, 1990.
(23) Holbrook, K. A. Pilling, M. J. Robertson, S. H. *Unimolecular Reactions*; Wiley: New York, 1996.
(24) Loh, S. K.; Hales, D. A.; Lian, L.; Armentrout, P. B. *J. Chem. Phys.* **1989**, *90*, 5466.
(25) Khan, F. A.; Clemmer, D. E.; Schultz, R. H.; Armentrout, P. B. *J. Phys. Chem.* **1993**, *97*, 7979.
(26) Rodgers, M. T.; Ervin, K. M.; Armentrout, P. B. *J. Chem. Phys.* **1997**, *106*, 4499.
(27) Armentrout, P. B. *J. Chem. Phys.* **2007**, *126*, 234302.
(28) Frisch, M. J. et al. *Gaussian 03*, Rev. B.02; Gaussian, Inc.: Pittsburgh, PA, 2003.
(29) Becke, A. D. *J. Chem. Phys.* **1993**, *98*, 5648.
(30) Lee, C.; Yang, W.; Parr, R. G. *Phys. Rev. B* **1988**, *37*, 785.
(31) Ditchfield, R.; Hehre, W. J.; Pople, J. A. *J. Chem. Phys.* **1971**, *72*, 5639.
(32) Bauschlicher, C. W., Jr.; Partridge, H. *J. Chem. Phys.* **1995**, *103*, 1788.
(33) Perdew, J. P. *Phys. Rev. B* **1986**, *33*, 1788.
(34) Moller, C.; Plesset, M. S. *Phys. Rev. B* **1934**, *46*, 618.
(35) Dalleska, N. F.; Honma, K.; Armentrout, P. B. *J. Am. Chem. Soc.* **1993**, *115*, 12125.
(36) O'Brien, J. T.; Williams, E. R. *J. Phys. Chem. A* **2008**, *112*, 5893.
(37) Duncombe, B. J.; Duale, K.; Buchanan-Smith, A.; Stace, A. J. *J. Phys. Chem. A* **2007**, *111*, 5158.

JP906241Q